Sensing-Throughput Tradeoff for Cognitive Radio as Interweave System: A Deployment-Centric Viewpoint

Ankit Kaushik[*], *Student Member, IEEE*,
Shree Krishna Sharma[†], *Member, IEEE*, Symeon Chatzinotas[†], *Senior Member, IEEE*,
Björn Ottersten[†], *Fellow, IEEE*, Friedrich K. Jondral[*] *Senior Member, IEEE*

Abstract

Cognitive Radio is envisaged as one of the potential candidates that addresses the issue of spectrum scarcity. Secondary access to the licensed spectrum is viable only if the interference is avoided at the primary system. In this regard, different paradigms have been conceptualized in the existing literature. Of these, Interweave Systems (ISs) that employ spectrum sensing have been widely investigated. This makes performance characterization of a cognitive radio system critical, hence, an interesting research problem. Baseline models investigated in the literature characterize the performance of IS in terms of sensing-throughput tradeoff, however, this characterization assumes the knowledge of the involved channels at secondary transmitter, which is unavailable in practice. As a result, these models depict an ideal scenario, thereby making the performance characterization based on these models disputable and impractical for hardware deployment. Motivated by this fact, we establish a novel model that incorporates channel estimation in the system model, and consequently investigate the impact of estimation on the performance of IS. More particularly, the variation induced in the probability of detection affects the detector performance at the secondary transmitter, that may result in severe interference at the primary users. In this view, we propose to employ two constraints namely, average and outage constraints on the probability of detection, in order to capture the performance of the IS while considering the variation

[*] A. Kaushik and F. K. Jondral are with Communications Engineering Lab, Karlsruhe Institute of Technology (KIT), Germany. Email:{ankit.kaushik,friedrich.jondral}@kit.edu.

[†] S.K. Sharma, S. Chatzinotas and B. Ottersten are with SnT - securityandtrust.lu, University of Luxembourg, Luxembourg. Email:{shree.sharma, symeon.chatzinotas, bjorn.ottersten}@uni.lu.

The preliminary analysis of this paper has been presented at CROWNCOM 2015 in Doha, Qatar [1].

induced due to the imperfect channel estimation. Our analysis reveals that the ideal scenario considerably overestimates the performance of the IS. Finally, it is shown that with an appropriate choice of the estimation time determined by the proposed model, the degradation in performance of the IS can be effectively controlled, and subsequently enhances the achievable throughput of the deployed hardware.

I. Introduction

We are currently in the phase of conceptualizing the requirements of the fifth-generation (5G) of wireless standards. One of the major requirements includes the improvement in the areal capacity (bits/s/m^2) by a factor of 1000 [2]. A large contribution of this demand is procured by means of an extension to the existing spectrum. Recently, the spectrum beyond 6 GHz largely entails the millimeter wave is envisaged as a powerful source of spectrum for the 5G systems. However, the millimeter wave technology is still in its nascent stage and along with complex regulatory requirements in this regime, it is surmounted by key-challenges like propagation loss, low efficiency of radio frequency components such as power amplifiers, size of the antenna and link acquisition that need to be addressed [3]. Therefore, to capture a deeper insight of its feasibility in 5G, it is essential to overcome the aforementioned challenges in the forthcoming future.

In contrast to that, the spectrum below 6 GHz, which is appropriate especially for mobile communications, presents an alternative solution. Due to its static allocation, this spectrum is on the verge of depletion. However, it is possible to overcome this scarcity if we manage to utilize this radio spectrum efficiently. In this perspective, Cognitive Radio (CR) is foreseen as one of the potential contender that addresses the problem of spectrum scarcity. Over the past one and a half decade, the notion of CR has evolved at a tremendous pace right from its origin by Mitola *et al.* in 1999 [4] and consequently, it has acquired certain maturity. However, from a deployment perspective, this technology is still in its preliminary phase. In this view, it is imperative to make substantial efforts that enable the disposition of this concept over a hardware platform.

An access to the licensed spectrum is an outcome to the paradigm employed by the Secondary User (SU). Based on the paradigms described in the literature, all CR systems that provide dynamic access to the spectrum fall mainly under three categories, namely, interweave, underlay and overlay systems [5]. In Interweave Systems (IS), the SUs render an interference-free access to the licensed spectrum by exploiting spectral holes in different domains such as time, frequency, space and polarization existing in the licensed spectrum, whereas underlay systems enable an interference-tolerant access under which the SUs are allowed to use the licensed spectrum as long as they respect the interference constraints of the Primary Receivers (PRs). Besides that, overlay systems consider participation of higher layers for enabling spectral coexistence between two or more wireless networks. However, IS is mostly preferred not only for performing theoretical analysis but for practical implementation as well. Motivated by these facts, this paper focuses on the performance analysis of the ISs from a deployment perspective.

Motivation and Related Work

Spectrum sensing is an integral part of the IS. At the Secondary Transmitter (ST), sensing is necessary for detecting the presence or absence of a primary signal, thereby protecting the PRs against harmful interference. Sensing at the ST is accomplished by listening to the signal transmitted by the Primary Transmitter (PT). For detecting a primary signal, several techniques such as energy detection, matched filtering, cyclostationary and feature-based detection exist [6], [7]. Because of its versatility towards unknown primary signals and its low computational as well as deployment complexity requirement, energy detection has been extensively investigated in the literature [8]–[12]. According to energy detection, the decision is accomplished by comparing the power received at the ST to a threshold. In reality, the ST encounters variation in the received power due to existence of thermal noise at the receiver and fading in the channel. This leads to sensing errors described as misdetection or false alarm, thus, limiting the performance of the IS. In order to determine the performance of the detector, it is essential to characterize the expressions of probability of detection and probability of false alarm.

In particular, probability of detection is critical for the primary system because it protects the PR from the interference induced by the ST. As a result, sustaining a target of probability of detection is of paramount importance to the secondary system [13]. Therefore, the characterization of the probability of detection becomes absolutely necessary for the performance analysis of the IS. In this context, Urkowitz [8] introduced a probabilistic model that establishes a fundamental framework for characterizing the sensing errors, however, the characterization accounted only for noise in the system. To encounter the variation because of fading in the channel, a frame structure is introduced such that the channel is considered to remain constant over the frame duration, however, upon exceeding the frame duration, the system may witness a different realization of the channel. Based on this frame structure, the performance of the IS has been investigated as *short-term* [14]–[16] and *long-term* [9]–[11] characterization.

The long-term characterization is a classical approach that applies a fading model to average out the variation in the received power. Subject to the deployment scenario[1], different fading models –

[1]These scenarios include urban, suburban and rural or indoor and outdoor from a different perspective.

Rice, Rayleigh, Nakagami-m and Log-normal can be employed [17]. The analytical expressions for the expected probability of detection for these fading models are characterized in [9]–[11]. Considering a CR system, this approach has some major drawbacks. Fading models depict a long-term characterization of the system, however, short-term interference that may lead to outage is ignored, thereby deteriorating the performance of a primary system. Moreover, fading models are specific to the deployment scenario, hence, the knowledge of the fading model is necessary while designing a CR system. Apart from that, every fading model incurs certain model parameters. As a result, estimation of these parameters at the ST [18], particularly during the initial phase of the deployment, imposes an additional overhead on the secondary system. In practice, due to mobility, most systems are likely to violate stationarity over a long duration. Thus, it becomes challenging to track these model parameters. As a consequence, these drawbacks constrict the applicability of this approach to practical CR systems.

To overcome these aforementioned drawbacks, an alternative approach that considers the short-term characterization is established [14]–[16] such that the performance is analyzed for a single frame[2]. In this way, unlike long-term approach, we preclude the variation due to the channel and consider the variation due to noise in the system. Subsequently, this approach eludes the deployment of the fading model and model complexities thereafter. Motivated by these facts, we focus on the short-term approach for performance analysis.

Problem Formulation

Recently, the performance characterization of CR systems in terms of sensing-throughput tradeoff has received significant attention [14], [16], [19], [20]. According to Liang *et al.* [14], the ST assures a reliable detection of a primary signal, thereby sustaining the probability of detection above a desired level with an objective of optimizing the throughput at the Secondary Receiver (SR). In this way, the sensing-throughput tradeoff renders a suitable sensing time that achieves an optimum throughput for a given received power. However, to characterize the probability of detection and throughput, the system requires the knowledge of interacting channels, namely, a *sensing* channel, an *access* channel and an *interference* channel, cf. Fig. 1[3]. Several contributions investigated in the literature assume this knowledge to be available at the

[2] By single frame, we refer to the statistical realizations of the received power, whereas [14]–[16] consider the temporal realizations of the same across several frames, also described as the path loss model. Considering ergodic behaviour of the noise, the performance characterization under these two scenarios are equivalent.

[3] As the interference to the PR is controlled by regulatory constraint over the probability of detection, in this view, the interaction with the PR is excluded in the scenario [14].

ST. In reality, the knowledge of these channels is not available, thus, needs to be estimated at the ST. As a result, the existing solutions are considered idealistic for performing analysis, however, they are not suitable for deployment.

Following the above discussion, it is apparent that received power, that entails the sensing channel, is crucial for characterizing the probability of detection, therefore, is essential for evaluating the detector's performance. The channel, according to the short-term characterization, is regarded as unknown and expected to remain constant over a frame duration, hence, it is reasonable to include received power estimation for each frame [1]. Inherent to the estimation process, a variation is induced in the probability of detection. In this sense, characterizing the performance of a detector with received power estimation remains an open problem. Besides probability of detection, probability of false alarm largely accounts for the throughput attained by the secondary system at the SR. The characterization of the probability of false alarm requires the knowledge of the noise power. Subject to a given uncertainty [21], this knowledge can be acquired through hardware calibration. In parallel to that, the variation in the probability of detection further translates to the variation in the secondary throughput. Moreover, the estimation of the access and the interference channels impose an additional variation on the throughput. Hence, to characterize the performance of the IS in terms of sensing-throughput tradeoff, it is essential to capture these variations in the system.

In order to overcome these bottlenecks, the following strategy is employed in this paper. Firstly, we consider received power estimation at the ST that allows us to constrain the probability of detection at a desired level. However, with the inclusion of estimation, the system anticipates: (i) a performance loss in terms of temporal resources used and (ii) a variation in the performance parameters due to imperfect estimation. A preliminary analysis of this performance loss was carried out in [1], where, it was revealed that at low signal to noise ratio regime, imperfect estimation of received power corresponds to large variation in probability of detection, hence, causing a severe degradation in the performance of the IS. However, the performance degradation was determined by means of lower and upper bounds. In this work, we consider a more exact analysis, whereby we capture the variation in probability of detection by characterizing its distribution function. Using this, we apply new probabilistic constraints on the probability of detection that allow IS to operate at low signal to noise ratio.

Besides that, we include channel estimation at the SR to acquire the knowledge of the access and interference channels. It is well-known that systems with transmitter information (such as matched filter, pilot symbols, modulation type and time-frequency synchronization) at the receiver acquire channel knowledge by listening to the pilot data sent by the ST [22]–[25]. Other systems, where the receiver

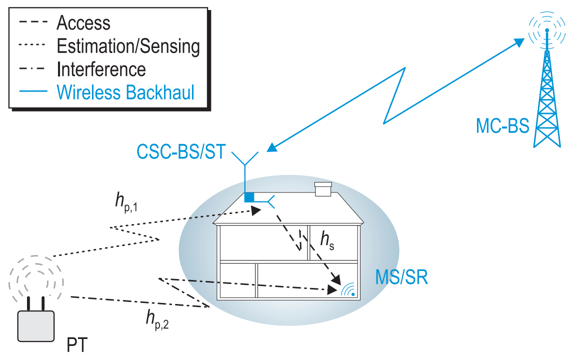

Fig. 1. A cognitive small cell scenario demonstrating: (i) the interweave paradigm, (ii) the associated network elements, which constitute Cognitive Small Cell-Base Station/Secondary Transmitter (CSC-BS/ST), Mobile Station/Secondary Receiver (MS/SR), Macro Cell-Base Station (MC-BS) and Primary Transmitter (PT), (iii) the interacting channels: sensing, access and interference channel.

possesses either no access to this information or limited by hardware complexity, procure channel knowledge indirectly by estimating a different parameter, for instance, received signal strength or received power, that entails the channel knowledge. Recently, pilot based estimation [26], [27] and received power estimation [28] have been applied to obtain channel knowledge and depict the performance of CR systems. However, the analysis was restricted to underlay systems, where the emphasis was laid on modelling the interference at the PR. In this paper, we extend this concept to the IS, hence, employ pilot based estimation for the access channel and received power based estimation for the sensing and interference channels, cf. Fig. 1. Upon acquiring the knowledge of these channels at the ST, we depict the impact of imperfect channel estimation on the performance of the IS in terms of sensing-throughput tradeoff. Unlike the sensing channel, the access and interference channels have to be estimated at the SR and made available at the ST through a feedback channel.

Contributions

The major contributions of this paper can be summarized as follows:

- The main goal of the paper is to establish a system model that constitutes estimation of: (i) sensing channel at the ST, (ii) access and (iii) interference channels at the SR. With the inclusion of estimation, the system witnesses variation in the performance parameters and a certain performance loss. Based on the proposed model, this work investigates these two aspects and characterizes the true performance of the IS.

- To capture the variation induced in the system, we characterize the distribution functions of performance parameters, such as, probability of detection and capacities at the SR. More importantly, we utilize the distribution function for the probability of detection to establish an average constraint or an outage constraint as new Primary User (PU) constraints on the probability of detection.
- Subject to the new constraints, we establish the expressions of sensing-throughput tradeoff to capture the variation in the performance parameters and evaluate the performance loss in terms of the optimum throughput in the IS.
- Finally, we depict a fundamental tradeoff between estimation time, sensing time and achievable throughput. We exploit this tradeoff to determine a suitable estimation and sensing time that depicts an optimal performance of the IS.

Organization

The subsequent sections of the paper are organized as follows: Section II describes the system model that includes the deployment scenario, the signal model and the performance characterization for the ideal scenario for the IS. Section III presents the proposed model that incorporates channel estimation and characterizes the distribution functions of the performance parameters. Section IV establishes the sensing-throughput tradeoff subject to average and outage constraints. Section V analyzes the numerical results based on the obtained expressions. Finally, Section VI concludes the paper. Table I lists the definitions of acronyms and mathematical notations used in the paper.

II. System Model

Deployment Scenario

Cognitive Small Cell (CSC), a CR application, characterizes a small cell deployment that fulfills the spectral requirements for Mobile Stations (MSs) operating indoor, cf. Fig. 1. For the disposition of the CSC in the network, the following key elements are essential: a CSC-Base Station (CSC-BS), a Macro Cell-Base Station (MC-BS) and MS, cf. Fig. 1. MSs are the indoor devices served by the CSC-BS over an access channel. Furthermore, the MC-BS is connected to several CSC-BSs over a wireless backhaul [4]. Moreover, the transmissions from the PT to the CSC-BS and the MS can be listened over sensing and interference channel. Although the MC-BS and the MS already exist in the conventional

[4]A wireless backhaul is a point-to-point wireless link between the CSC-BS and MC-BS that relays the traffic generated from the CSC to the core network.

TABLE I

DEFINITIONS OF ACRONYMS AND NOTATIONS USED

Acronyms and Notations	**Definitions**
AC, OC	Average Constraint, Outage Constraint
CR	Cognitive Radio
CSC, CSC-BS, MC-BS, MS	Cognitive Small Cell, Cognitive Small Cell-Base Station, Macro Cell-Base Station, Mobile Station
IM, EM	Ideal Model, Estimation Model
IS	Interweave System
PU - PT, PR	Primary User - Primary Transmitter, Primary Receiver
SU - ST, SR	Secondary User - Secondary Transmitter, Secondary Receiver
$\mathcal{H}_1, \mathcal{H}_0$	Signal plus noise hypothesis, noise only hypothesis
f_{s}	Sampling frequency
$\tau_{\text{est}}, \tau_{\text{sen}}$	Estimation time, sensing time interval
T	Frame duration
$\text{P}_{\text{d}}, \text{P}_{\text{fa}}$	Probability of detection, probability of false alarm
$\bar{\text{P}}_{\text{d}}$	Target probability of detection
κ	Outage Constraint over probability of detection
$h_{\text{p,1}}, h_{\text{p,2}}, h_{\text{s}}$	Channel coefficient for the link PT-ST, PT-SR, ST-SR
$\gamma_{\text{p,1}}, \gamma_{\text{p,2}}, \gamma_{\text{s}}$	Signal to noise ratio for the link PT-ST, PT-SR, ST-SR
R_{s}	Throughput at SR
C_0, C_1	Shanon capacity at SR without and with interference from PT
μ	Threshold for the energy detector
$F_{(\cdot)}$	Cumulative distribution function of random variable $(\cdot)$
$f_{(\cdot)}$	Probability density function of random variable $(\cdot)$
$\hat{(\cdot)}$	Estimated value of $(\cdot)$
$\tilde{(\cdot)}$	Optimum value of $(\cdot)$
$\mathbb{E}_{(\cdot)}$	Expectation with respect $(\cdot)$
$\mathbb{P}$	Probability measure
$\mathbf{T}(\cdot)$	Test statistics
$x_{(\cdot)}[n], y_{(\cdot)}[n]$	n^{th} sample of the transmitted discrete and real signal, received discrete and real signal at $(\cdot)$
$P_{\text{Tx, }(\cdot)}, P_{\text{Rx, }(\cdot)}$	Power transmitted, power received at $(\cdot)$
σ_x^2, σ_w^2	Signal variance at PT, noise variance at ST and SR
$\Gamma(\cdot)$	Gamma function
$\Gamma(\cdot, \cdot)$	Regularized incomplete upper Gamma function
$\Gamma^{-1}(\cdot, \cdot)$	Inverse of regularized incomplete upper Gamma function
$\mathcal{N}, \mathcal{X}^2, \mathcal{X}_1^2$	Normal, central chi-squared, non-central chi-squared distribution
N_{s}	Number of pilot symbols used for pilot based estimation at the SR for h_{s}
$N_{\text{p,2}}$	Number of samples used for received power estimation at the SR for $h_{\text{p,2}}$
a_1, b_1, a_2, b_2	Model parameters of Gamma distribution
λ	Non-centrality parameter of $\mathcal{X}_1^2$ distribution

cellular architecture, to incorporate the opportunistic access inside the CSC, it is necessary to consider a functionality upgrade. Considering the fact that the IS is employed at the CSC-BS, the CSC-BS and the MS represents the ST and SR, respectively. In [29], the challenges involved while deploying the CSC as IS were presented. For simplification, a PU constraint based on probability of false alarm rate was considered in the system model. With the purpose of improving system's reliability, we extend the analysis to employ a PU constraint on the probability of detection. As a follow-on from the ideal model depicted in [14], we consider a slotted medium access for the IS, where the time axis is segmented into frames of length T. According to which, the ST employs periodic sensing, hence, each frame consists of a sensing slot τ_{sen} and the remaining duration $T - \tau_{\text{sen}}$ is utilized for data transmission. For small T relative to the PU's expected ON/OFF period, the requirement of the ST to be in alignment to PUs' medium access can be relaxed [30]–[32].

Signal model

Subject to the underlying hypothesis that illustrates the presence $(\mathcal{H}_1)$ or absence $(\mathcal{H}_0)$ of primary signal, the discrete and real signal received at the ST is given by

$$y_{\text{ST}}[n] = \begin{cases} h_{\text{p,1}} \cdot x_{\text{PT}}[n] + w[n] & : \mathcal{H}_1 \\ w[n] & : \mathcal{H}_0 \end{cases}, \tag{1}$$

where $x_{\text{PT}}[n]$ corresponds to a discrete and real sample transmitted by the PT, $|h_{\text{p,1}}|^2$ represents the power gain of the sensing channel for a given frame and $w[n]$ is Additive White Gaussian Noise (AWGN) at the ST. In the literature [14], the primary signal $x_{\text{PT}}[n]$ can be modelled as: (i) PSK modulated signal, or (ii) Gaussian signal. The signals that are prone to high inter symbol interference or entail precoding can be modelled as Gaussian signals. For this paper, we focus our analysis on the latter case. As a result, the mean and variance for the signal and noise are determined as $\mathbb{E}\left[x_{\text{PT}}[n]\right] = 0$, $\mathbb{E}\left[w[n]\right] = 0$, $\mathbb{E}\left[|x_{\text{PT}}[n]|^2\right] = \sigma_x^2$ and $\mathbb{E}\left[|w[n]|^2\right] = \sigma_w^2$. The channel $h_{\text{p,1}}$ is considered to be independent to $x_{\text{PT}}[n]$ and $w[n]$, thus, y_{ST} is also an independent and identically distributed (i.i.d.) random process.

Similar to (1), during data transmission, the discrete and real received signal at the SR conditioned over the probability of detection (P_d) and probability of false alarm (P_fa) is given by

$$y_{\text{SR}}[n] = \begin{cases} h_{\text{s}} \cdot x_{\text{ST}}[n] + h_{\text{p,2}} \cdot x_{\text{PT}}[n] + w[n] & : 1 - \text{P}_\text{d} \\ h_{\text{s}} \cdot x_{\text{ST}}[n] + w[n] & : 1 - \text{P}_\text{fa} \end{cases}, \tag{2}$$

where $x_{\text{ST}}[n]$ corresponds to discrete and real sample transmitted by the ST. Further, $|h_{\text{s}}|^2$ and $|h_{\text{p,2}}|^2$ represent the power gains for access and interference channels, cf. Fig. 1.

Sensing

Following the frame structure, ST performs sensing for a duration of τ_{sen}. The test statistics $\mathrm{T}(\mathbf{y})$ at the ST is evaluated as

$$\mathrm{T}(\mathbf{y}) = \frac{1}{\tau_{\text{sen}} f_{\text{s}}} \sum_{n}^{\tau_{\text{sen}} f_{\text{s}}} |y_{\text{ST}}[n]|^2 \underset{\mathcal{H}_0}{\overset{\mathcal{H}_1}{\gtrless}} \mu, \tag{3}$$

where μ is the threshold and $\mathbf{y}$ is a vector with $\tau_{\text{sen}} f_{\text{s}}$ samples. $\mathrm{T}(\mathbf{y})$ represents a random variable, whereby the characterization of the distribution function depends on the underlying hypothesis. Corresponding to $\mathcal{H}_0$ and $\mathcal{H}_1$, $\mathrm{T}(\mathbf{y})$ follows a central chi-squared ($\mathcal{X}^2$) distribution [33]. As a result, the probability of detection ($\mathrm{P_d}$) and the probability of false alarm ($\mathrm{P_{fa}}$) corresponding to (3) are determined as [21]

$$\mathrm{P_d}(\mu, \tau_{\text{sen}}, P_{\text{Rx,ST}}) = \Gamma\left(\frac{\tau_{\text{sen}} f_{\text{s}}}{2}, \frac{\tau_{\text{sen}} f_{\text{s}} \mu}{2 P_{\text{Rx,ST}}}\right), \tag{4}$$

$$\mathrm{P_{fa}}(\mu, \tau_{\text{sen}}) = \Gamma\left(\frac{\tau_{\text{sen}} f_{\text{s}}}{2}, \frac{\tau_{\text{sen}} f_{\text{s}} \mu}{2 \sigma_w^2}\right), \tag{5}$$

where $\Gamma(\cdot,\cdot)$ represents a regularized upper Gamma function [34].

Sensing-Throughput tradeoff

Following the characterization of $\mathrm{P_{fa}}$ and $\mathrm{P_d}$, Liang *et. al.* [14] established a tradeoff between the sensing time and secondary throughput (R_{s}) attained subject to a target probability of detection ($\bar{\mathrm{P}}_{\text{d}}$). This tradeoff is represented as

$$\tilde{R}_{\text{s}}(\tilde{\tau}_{\text{sen}}) = \max_{\tau_{\text{sen}}} R_{\text{s}}(\tau_{\text{sen}}) = \frac{T - \tau_{\text{sen}}}{T}\Big[\mathrm{C}_0(1 - \mathrm{P_{fa}})\mathbb{P}(\mathcal{H}_0) + \mathrm{C}_1(1 - \mathrm{P_d})\mathbb{P}(\mathcal{H}_1)\Big], \tag{6}$$

$$\text{s.t. } \mathrm{P_d} \geq \bar{\mathrm{P}}_{\text{d}}, \tag{7}$$

$$\text{where } \mathrm{C}_0 = \log_2\left(1 + |h_{\text{s}}|^2 \frac{P_{\text{Tx,ST}}}{\sigma_w^2}\right) = \log_2(1 + \gamma_{\text{s}}) \tag{8}$$

$$\text{and } \mathrm{C}_1 = \log_2\left(1 + \frac{|h_{\text{s}}|^2 P_{\text{Tx,ST}}}{|h_{\text{p,2}}|^2 P_{\text{Tx,PT}} + \sigma_w^2}\right) = \log_2\left(1 + \frac{|h_{\text{s}}|^2 P_{\text{Tx,ST}}}{P_{\text{Rx,SR}}}\right) = \log_2\left(1 + \frac{\gamma_{\text{s}}}{\gamma_{\text{p,2}} + 1}\right), \tag{9}$$

where $\mathbb{P}(\mathcal{H}_0)$ and $\mathbb{P}(\mathcal{H}_1)$ are the probabilities of occurrence for the respective hypothesis, whereas $\gamma_{\text{p,2}}$ and γ_{s} correspond to signal to noise ratio for the links PT-SR and SR-SR, respectively. In other words, using (6), the ST determines a suitable sensing time $\tau_{\text{sen}} = \tilde{\tau}_{\text{sen}}$, such that the throughput is optimized ($\tilde{R}_{\text{s}}$) subject to a target probability of detection, cf. (7). From the deployment perspective, the tradeoff depicted above has the following fundamental issues:

- Without the knowledge of the received power (sensing channel), it is not feasible to characterize $\mathrm{P_d}$. This leaves the characterization of the throughput (6) impossible and the constraint defined in (7) inappropriate.
- Moreover, the knowledge of the interacting channels is required at the ST, cf. (8) and (9) for characterizing the throughput in terms of $\mathrm{C_0}$ and $\mathrm{C_1}$ at the SR.

Taking into account these issues, it is impractical to depict the performance of IS based on the ideal model, mentioned above. In the subsequent section, we propose an estimation model that addresses these issues, thereby including the estimation of the sensing channel at the ST and interference and access channels at the SR. Based on the proposed model, we then investigate the performance of the IS in terms of the sensing-throughput tradeoff.

III. Proposed Model

The inclusion of estimation of the interacting channels causes variation in the parameters $\mathrm{P_d}$, $\mathrm{C_0}$ and $\mathrm{C_1}$. Unless characterized, this variation may seriously degrade the performance of the hardware deployed. In this view, we include the estimation of the interacting channels in the system model, thereby characterizing the variation in $\mathrm{P_d}$, $\mathrm{C_0}$ and $\mathrm{C_1}$ by means of distribution functions. By utilizing these expressions, we finally obtain a characterization of sensing-throughput tradeoff. To include channel estimation, we propose a frame structure that constitutes estimation τ_{est}, sensing τ_{sen} and data transmission $T-(\tau_{\mathrm{est}}+\tau_{\mathrm{sen}})$, where $\tau_{\mathrm{est}}, \tau_{\mathrm{sen}}$ correspond to time intervals and $\tau_{\mathrm{est}} + \tau_{\mathrm{sen}} < T$, cf. Fig. 2. In practice, the estimated values of the interacting channels are required for determining the suitable sensing time, hence, the sequence depicted in Fig. 2, whereby estimation is followed by sensing is reasonable for the hardware deployment. Besides that, particularly for sensing channel, the samples used for estimation can be combined with the samples acquired for sensing, thereby improving the performance of the detector at the ST, this however, complicates the analytical tractability of the distribution function of the probability of detection. Hence, to simplify the analysis, in this work, we consider ~~the~~ τ_{est} and τ_{sen} as disjoint events in time. In this regard, the derived expressions based on our proposed model represents a lower performance bound. Next, in the following subsections, we present the estimation of the interacting channels.

Estimation of sensing channel ($h_{p,1}$)

Following the previous discussions, the ST acquires the knowledge of $h_{\mathrm{p,1}}$ by estimating its received power. The estimated received power is required for the characterization of $\mathrm{P_d}$, thereby evaluating the detector performance.

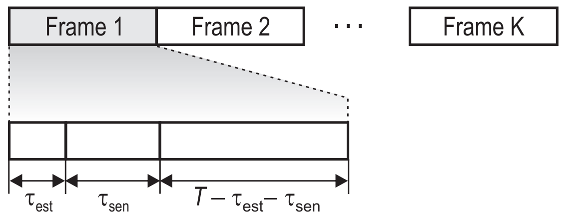

Fig. 2. Frame structure of interweave system with received power estimation.

Under $\mathcal{H}_1$, the received power estimated during the estimation phase at the ST is given as [8]

$$\hat{P}_{\text{Rx,ST}} = \frac{1}{\tau_{\text{est}} f_{\text{s}}} \sum_{n}^{\tau_{\text{est}} f_{\text{s}}} |y_{\text{ST}}[n]|^2. \tag{10}$$

$\hat{P}_{\text{Rx,ST}}$ determined in (10) using $\tau_{\text{est}} f_{\text{s}}$ samples follows a central chi-squared distribution $\mathcal{X}^2$ [33]. The cumulative distribution function of $\hat{P}_{\text{Rx,ST}}$ is given by

$$F_{\hat{P}_{\text{Rx,ST}}}(x) = \Gamma\left(\frac{\tau_{\text{est}} f_{\text{s}}}{2}, \frac{\tau_{\text{est}} f_{\text{s}} x}{2 P_{\text{Rx,ST}}}\right). \tag{11}$$

Estimation of access channel (h_s)

The signal received from the ST undergoes matched filtering and demodulation at the SR, hence, it is reasonable to employ pilot based estimation for h_{s}. Unlike received power estimation, pilot based estimation renders a direct estimation of the channel. Now, to accomplish pilot based estimation, the SR aligns itself to pilot symbols transmitted by the ST. Under $\mathcal{H}_1$, the discrete and real pilot symbols at the output of the demodulator is given by [24]

$$p[n] = \sqrt{E_{\text{s}}} h_{\text{s}} + w[n], \tag{12}$$

where E_{s} denotes the pilot energy. Without loss of generality, the pilot symbols are considered to be +1. The maximum likelihood estimate, representing a sample average of N_{s} pilot symbols, is given by [23]

$$h_{\text{s}} = \hat{h}_{\text{s}} + \underbrace{\frac{\sum_{i}^{N_{\text{s}}} n[i]}{2 N_{\text{s}}}}_{\epsilon}, \tag{13}$$

where ϵ denotes the estimation error. The estimate $\hat{h}_{\text{s}}$ is unbiased, efficient and achieves a Cramer-Rao bound with equality, with variance $\mathbb{E}\left[|h_{\text{s}} - \hat{h}_{\text{s}}|^2\right] = \sigma_w^2/(2N_{\text{s}})$ [24]. Consequently, $\hat{h}_{\text{s}}$ conditioned on h_{s} follows a Gaussian distribution.

$$\hat{h}_{\text{s}} | h_{\text{s}} \sim \mathcal{N}\left(h_{\text{s}}, \frac{\sigma_w^2}{2 N_{\text{s}}}\right). \tag{14}$$

As a result, the power gain $|\hat{h}_\mathrm{s}|^2$ follows a non-central chi-squared ($\mathcal{X}_1^2$) distribution with 1 degree of freedom and non-centrality parameter $\lambda = \frac{|h_\mathrm{s}|^2}{\frac{\sigma_w^2}{2N_\mathrm{s}}}$.

Estimation of interference channel ($h_{p,2}$)

In addition, analog to sensing channel, the SR performs received power estimation by listening to the transmission from the PT. The knowledge of $h_\mathrm{p,2}$ is required to characterize interference from the PT. Under $\mathcal{H}_0$, the discrete signal model at the SR is given as

$$y_\mathrm{SR}[n] = h_\mathrm{p,2} \cdot x_\mathrm{PT}[n] + w[n]. \tag{15}$$

The received power at the SR from the PT given by

$$\hat{P}_\mathrm{Rx,SR} = \frac{1}{N_\mathrm{p,2}} \sum_{n}^{N_\mathrm{p,2}} |y_\mathrm{SR}[n]|^2, \tag{16}$$

follows a $\mathcal{X}^2$ distribution, where $N_\mathrm{p,2}$ corresponds to the number of samples used for estimation.

Assumptions and Approximations

To simplify the analysis and sustain analytical tractability for the proposed model, several assumptions considered in the paper are summarized as follows:

- We consider that all transmitted signals are subjected to distance dependent path loss and small scale fading gain. With no loss of generality, we consider that the channel gains include distance dependent path loss and small scale gain. Moreover, the coherence time for the channel gain is considered to be greater than the frame duration[5].
- To ensure mathematical tractability of the proposed model, we consider disjoint sets of samples for estimation and sensing for a certain frame. However, in practice, it is possible to utilize the samples used in the estimation phase for sensing purpose as well, which leads to an improvement in the performance in terms of the number of samples utilized for sensing.
- We assume perfect knowledge of the noise power in system, however, the uncertainty in noise power can be captured as a bounded interval [21]. Inserting this interval in the derived expressions, cf. Section IV, the performance of the IS can be expressed in terms of the upper and the lower bounds.

[5]In the scenarios where the coherence time exceeds the frame duration, in such cases our characterization depicts a lower performance bound.

- For all degrees of freedom, $\mathcal{X}_1^2$ distribution can be approximated as Gamma distribution [35]. The parameters of the Gamma distribution are computed by comparing its first two central moments with those of $\mathcal{X}_1^2$.
- In addition, the system model stipulates the knowledge of the underlying hypothesis at the ST and the SR. Upon the application of PU traffic models proposed in [30]–[32], it is possible to acquire this knowledge with high probability. Moreover, it is reasonable that the ST and the SR perform estimation independently. Considering a realistic situation, it is possible that SR might not accomplish estimation in each frame, under such circumstances, the ST utilizes the previous estimation value for the analysis.
- Finally, it is assumed that the estimation time for the channels h_{s} and $h_{\mathrm{p,2}}$ is smaller than $h_{\mathrm{p,1}}$, that is $N_{\mathrm{p,2}}, N_{\mathrm{s}} < \tau_{\mathrm{sen}} f_{\mathrm{s}}$. Hence, it is sufficient to incorporate $\max(\tau_{\mathrm{est}} f_{\mathrm{s}}, N_{\mathrm{s}}, N_{\mathrm{p,2}}) = \tau_{\mathrm{est}} f_{\mathrm{s}}$ in the expression of the throughput.

IV. Theoretical Analysis

At this stage, it is evident that the variation due to imperfect channel estimation translates to the variation of the performance parameters $\mathrm{P_d}, \mathrm{C}_0$ and C_1, which are fundamental to sensing-throughput tradeoff. Below, we capture this variation by characterizing their cumulative distribution functions $F_{\mathrm{P_d}}$, F_{C_0} and F_{C_1}, respectively.

Lemma 1: The cumulative distribution function of $\mathrm{P_d}$ is characterized as

$$F_{\mathrm{P_d}}(x) = 1 - \Gamma\left(\frac{\tau_{\mathrm{est}} f_{\mathrm{s}}}{2}, \frac{\tau_{\mathrm{est}} f_{\mathrm{s}} \tau_{\mathrm{sen}} f_{\mathrm{s}} \mu}{4 P_{\mathrm{Rx,ST}} \Gamma^{-1}(\frac{\tau_{\mathrm{sen}}}{2}, x)}\right), \tag{17}$$

where $\Gamma^{-1}(\cdot,\cdot)$ is inverse function of regularized upper Gamma function [34].

Proof: The cumulative distribution function of $\mathrm{P_d}$ is defined as

$$F_{\mathrm{P_d}}(x) = \mathbb{P}(\mathrm{P_d} \leq x) \tag{18}$$

Using (4)

$$= \mathbb{P}\left(\Gamma\left(\frac{\tau_{\mathrm{sen}} f_{\mathrm{s}}}{2}, \frac{\tau_{\mathrm{est}} f_{\mathrm{s}} \mu}{2 \hat{P}_{\mathrm{Rx,ST}}}\right) \leq x\right) \tag{19}$$

$$= 1 - \mathbb{P}\left(\hat{P}_{\mathrm{Rx,ST}} \leq \frac{\mu \tau_{\mathrm{sen}} f_{\mathrm{s}}}{2\Gamma^{-1}\left(\frac{\tau_{\mathrm{sen}} f_{\mathrm{s}}}{2}, x\right)}\right) \tag{20}$$

Replacing the cumulative distribution function of $\hat{P}_{\mathrm{Rx,ST}}$ in (20), we obtain an expression of $F_{\mathrm{P_d}}$. ■

From (17), it is clearly observed that $F_{\mathrm{P_d}}$ depends on $P_{\mathrm{Rx,ST}}$, τ_{sen} and τ_{est}.

(a) $\tau_{\text{est}} \in \{1,5,10\}$ms and $\tau_{\text{sen}} = 1$ ms

(b) $\tau_{\text{est}} = 1$ ms and $\tau_{\text{sen}} \in \{1,5,10\}$ms

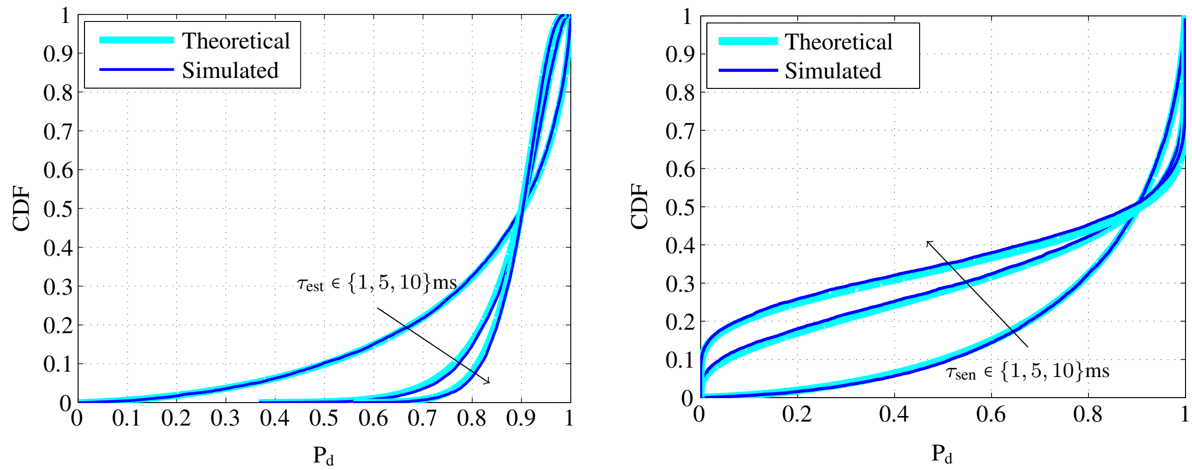

Fig. 3. CDF of $\mathrm{P_d}$ for different τ_{est} and τ_{sen}.

Lemma 2: The cumulative distribution function of $\mathrm{C_0}$ is defined as

$$F_{\mathrm{C_0}}(x) = \int_0^{\infty} f_{\mathrm{C_0}}(x)dx, \tag{21}$$

where

$$f_{\mathrm{C_0}}(x) = 2^x \ln 2 \frac{(2^x-1)^{a_1-1}}{\Gamma(a_1) b_1^{a_1}} \exp\left(-\frac{2^x-1}{b_1}\right), \tag{22}$$

and

$$a_1 = \frac{\left(\frac{\sigma_w^2}{2N_{\text{s}}}\frac{\sigma_w^2}{P_{\text{Tx,ST}}} + |h_{\text{s}}|^2\right)^2}{\frac{\sigma_w^2}{2N_{\text{s}}}\frac{\sigma_w^2}{P_{\text{Tx,ST}}}\left(2\frac{\sigma_w^2}{2N_{\text{s}}}\frac{\sigma_w^2}{P_{\text{Tx,ST}}} + 4|h_{\text{s}}|^2\right)} \text{ and } b_1 = \frac{\frac{\sigma_w^2}{2N_{\text{s}}}\frac{\sigma_w^2}{P_{\text{Tx,ST}}}\left(2\frac{\sigma_w^2}{2N_{\text{s}}}\frac{\sigma_w^2}{P_{\text{Tx,ST}}} + 4|h_{\text{s}}|^2\right)}{\left(\frac{\sigma_w^2}{2N_{\text{s}}}\frac{\sigma_w^2}{P_{\text{Tx,ST}}} + |h_{\text{s}}|^2\right)}. \tag{23}$$

Proof: Following the pdf of $|\hat{h}_{\text{s}}|^2$ in (14), the pdf $|\hat{h}_{\text{s}}|^2 \frac{P_{\text{Tx,ST}}}{\sigma_w^2}$ is given by

$$f_{\frac{|\hat{h}_{\text{s}}|^2 P_{\text{Tx,ST}}}{\sigma_w^2}}(x) = \frac{P_{\text{Tx,ST}}}{\sigma_w^2}\frac{1}{\frac{\sigma_w^2}{2N_{\text{s}}}}\frac{1}{2}\exp\left[-\frac{1}{2}\left(x\frac{\sigma_w^2}{2N_{\text{s}}}\frac{\sigma_w^2}{P_{\text{Tx,ST}}} + \lambda\right)\right]\left(\frac{x\frac{\sigma_w^2}{2N_{\text{s}}}}{\lambda}\frac{\sigma_w^2}{P_{\text{Tx,ST}}}\right)^{\frac{N_{\text{s}}}{4}-\frac{1}{2}}$$
$$I_{\frac{N_{\text{s}}}{2}-1}\left(\sqrt{\lambda x \frac{\sigma_w^2}{2N_{\text{s}}}\frac{\sigma_w^2}{P_{\text{Tx,ST}}}}\right).$$

Approximating $\mathcal{X}_1^2(\cdot,\cdot)$ with Gamma distribution $\Gamma(a_1, b_1)$ gives [35]

$$f_{\frac{|\hat{h}_{\text{s}}|^2 P_{\text{Tx,ST}}}{\sigma_w^2}} \approx \frac{1}{\Gamma(a_1)}\frac{x^{a_1-1}}{b_1^{a_1}}\exp\left(-\frac{x}{b_1}\right), \tag{24}$$

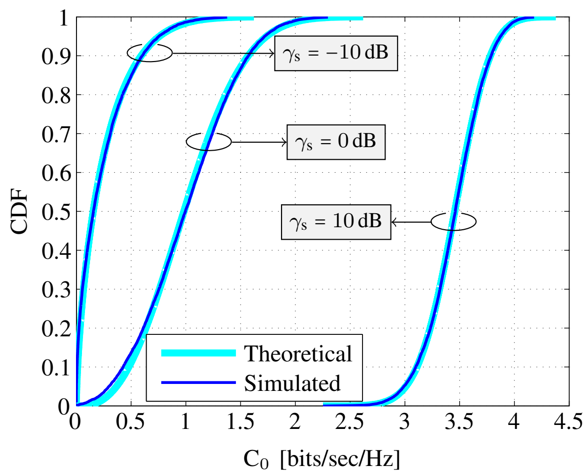

Fig. 4. CDF of C_0 for different values of $\gamma_s \in \{-10, 0, 10\}$dB.

where the parameters a_1 and b_1 in (24) are determined by comparing the first two central moments of the two distributions. Finally, by substituting the expression of C_0 in (8) yields (22). ■

Lemma 3: The cumulative distribution function of C_1 is given by

$$F_{C_1}(x) = \int_0^\infty f_{C_1}(x)dx, \tag{25}$$

where

$$f_{C_1}(x) = 2^x \ln 2 \frac{(2^x - 1)^{a_1-1}\Gamma(a_1 + a_2)}{\Gamma(a_1)\Gamma(a_2)b_1^{a_1} b_2^{a_2}} \left(\frac{1}{b_2} + \frac{2^x - 1}{b_1}\right), \tag{26}$$

and

$$a_2 = \frac{N_{p,2}}{2} \text{ and } b_2 = \frac{2P_{Rx,ST}}{\sigma_w^2 N_{p,2}}, \tag{27}$$

where a_1 and b_1 are defined in (23).

Proof: For simplification, we disintegrate the expression $\left(\frac{|\hat{h}_s|^2 P_{Tx,ST}}{\hat{P}_{Rx,SR}}\right)$ in (9), as $E_1 = \left(\frac{|\hat{h}_s|^2 P_{Tx,ST}}{\sigma_w^2}\right)$ and $E_2 = \left(\frac{\hat{P}_{Rx,SR}}{\sigma_w^2}\right)$, where $C_1 = \log_2\left(1 + \frac{E_1}{E_2}\right)$. The pdf of the expression E_1 is determined in (24).

Following the characterization $\hat{P}_{Rx,SR}$ in (16), the pdf of E_2 is determined as

$$f_{\frac{\hat{P}_{Rx,SR}}{\sigma_w^2}} = \frac{N_{p,2}\sigma_w^2}{P_{Rx,ST}} \frac{1}{2^{\frac{N_{p,2}}{2}}\Gamma\left(\frac{N_{p,2}}{2}\right)} \left(x\frac{N_{p,2}\sigma_w^2}{P_{Rx,ST}}\right)^{\frac{N_{p,2}}{2}-1} \exp\left(-x\frac{N_{p,2}\sigma_w^2}{2P_{Rx,ST}}\right). \tag{28}$$

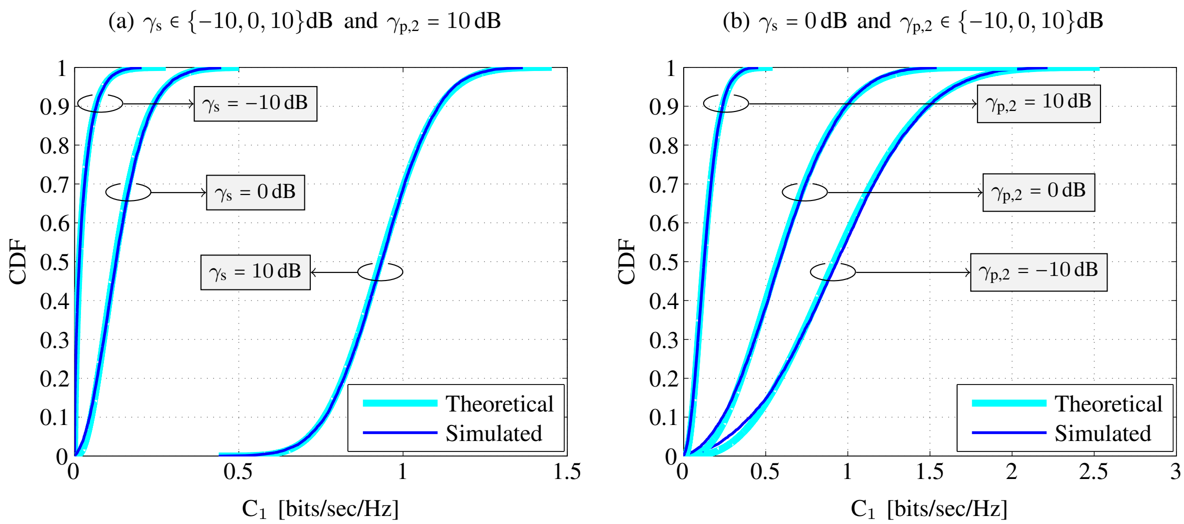

Fig. 5. CDF of C_1 for different γ_s and $\gamma_{p,2}$.

Using the characterizations of pdfs $f_{\frac{|\hat{h}_s|^2 P_{Tx,ST}}{\sigma_w^2}}$ and $f_{\frac{\hat{P}_{Rx,SR}}{\sigma_w^2}}$, we apply Mellin transform [36] to determine the pdf of $\frac{E_1}{E_2}$ as

$$f_{\frac{|\hat{h}_s|^2 P_{Tx,ST}}{\sigma_w^2} \Big/ \frac{\hat{P}_{Rx,SR}}{\sigma_w^2}}(x) = \frac{x^{a_1-1}\Gamma(a_1+a_2)}{\Gamma(a_1)\Gamma(a_2) b_1^{a_1} b_2^{a_2}} \left(\frac{1}{b_2} + \frac{x}{b_1}\right). \tag{29}$$

Finally, substituting the expression $\frac{E_1}{E_2}$ in C_1 yields (26). ■

Sensing-throughput tradeoff

Here, we establish sensing-throughput tradeoff for the estimation model that includes estimation time and incorporates variation in the performance parameter. Most importantly, by capturing this variation, we establish two new primary user constraints at the PR, namely, an average constraint and an outage constraint on the probability of detection. These constraints constrict the harmful interference at the PR. Based on these constraints and a certain choice of estimation time τ_{est}, we characterize the sensing-throughput tradeoff for the IS.

Theorem 1: Subject to an average constraint on P_d at the PR, the sensing-throughput tradeoff is given by

$$\begin{aligned} \tilde{R}_s(\tilde{\tau}_{sen}) = \max_{\tau_{sen}} \mathbb{E}_{P_d, C_0, C_1}\left[R_s(\tau_{sen})\right] = \frac{T - \tau_{sen} - \tau_{est}}{T} \Big[& \mathbb{E}_{C_0}\left[C_0\right](1 - P_{fa})\mathbb{P}(\mathcal{H}_0) + \\ & \mathbb{E}_{C_1}\left[C_1\right](1 - \mathbb{E}_{P_d}\left[P_d\right])\mathbb{P}(\mathcal{H}_1) \Big], \end{aligned} \tag{30}$$

$$\text{s.t. } \mathbb{E}_{\mathrm{P_d}}\left[\mathrm{P_d}\right] \le \bar{\mathrm{P}}_{\mathrm{d}}, \tag{31}$$

where $\mathbb{E}_{\mathrm{P_d}}[\cdot]$ represents the expectation with respect to $\mathrm{P_d}$, $\mathbb{E}_{\mathrm{P_d,C_0,C_1}}[\cdot]$ denotes the expectation with respect to $\mathrm{P_d}$, $\mathrm{C_0}$ and $\mathrm{C_1}$. Unlike (7), $\bar{\mathrm{P}}_{\mathrm{d}}$ in (30) represents the constraint on expected probability of detection.

Theorem 2: Subject to an outage constraint on $\mathrm{P_d}$ at the PR, the sensing-throughput tradeoff is given by

$$\tilde{R}_{\mathrm{s}}(\tilde{\tau}_{\mathrm{sen}}) = \max_{\tau_{\mathrm{sen}}} \mathbb{E}_{\mathrm{P_d,C_0,C_1}}\left[R_{\mathrm{s}}(\tau_{\mathrm{sen}})\right] = \frac{T-\tau_{\mathrm{sen}}-\tau_{\mathrm{est}}}{T}\Big[\mathbb{E}_{\mathrm{C_0}}\left[\mathrm{C_0}\right](1-\mathrm{P_{fa}})\mathbb{P}(\mathcal{H}_0)+$$

$$\mathbb{E}_{\mathrm{C_1}}\left[\mathrm{C_1}\right](1-\mathbb{E}_{\mathrm{P_d}}\left[\mathrm{P_d}\right])\mathbb{P}(\mathcal{H}_1)\Big], \tag{32}$$

$$\text{s.t. } \mathbb{P}(\mathrm{P_d} \le \bar{\mathrm{P}}_{\mathrm{d}}) \le \kappa, \tag{33}$$

where κ represents the outage constraint.

In order to solve the constrained optimization problems illustrated in Theorem 1 and Theorem 2, the following approach is considered. As a first step, an underlying constraint is employed to determine μ as a function of the τ_{sen} and τ_{est}. Its value is substituted in (4) and (5) to determine $\mathrm{P_{fa}}$ and $\mathrm{P_d}$. Finally, replacing $\mathrm{P_d}$ and $\mathrm{P_{fa}}$ in (30) and (32), we obtain an expression of the throughput in terms of τ_{sen}, τ_{est} and the system parameters. Using this expression, we consider the variation of expected throughput with τ_{est} and τ_{sen}, thereby determining an optimum throughput.

Corollary 1: For the average constraint, the expression $\mathbb{E}_{\mathrm{P_d}}\left[\mathrm{P_d}\right]$ in (31) did not lead to a closed form expression, consequently, no analytical expression of μ is obtained. In this context, we procure the μ for the average constraint numerically.

Corollary 2: For this case, we determine the μ based on the outage constraint. This is accomplished by combining the expression of $F_{\mathrm{P_d}}$ in (17) with the outage constraint (33)

$$P(\mathrm{P_d} \le \bar{\mathrm{P}}_{\mathrm{d}}) = F_{\mathrm{P_d}}(\bar{\mathrm{P}}_{\mathrm{d}}) \le \kappa. \tag{34}$$

Rearranging (34) gives

$$\mu \ge \frac{4P_{\mathrm{Rx,ST}}\Gamma^{-1}\left(1-\kappa, \frac{\tau_{\mathrm{est}} f_{\mathrm{s}}}{2}\right)\Gamma^{-1}\left(1-\bar{\mathrm{P}}_{\mathrm{d}}, \frac{\tau_{\mathrm{sen}} f_{\mathrm{s}}}{2}\right)}{\tau_{\mathrm{est}}\tau_{\mathrm{sen}}(f_{\mathrm{s}})^2}. \tag{35}$$

Upon replacing the respective thresholds in $\mathrm{P_d}$ and $\mathrm{P_{fa}}$ and evaluating the expectation over $\mathrm{P_d}$, $\mathrm{C_0}$ and $\mathrm{C_1}$ using the distribution functions characterized in Lemma 1, Lemma 2 and Lemma 3, we determine the expected throughput as a function of sensing and estimation time. As a consequence, for a certain estimation time, sensing-throughput tradeoff that depicts the variation of expected throughput against the

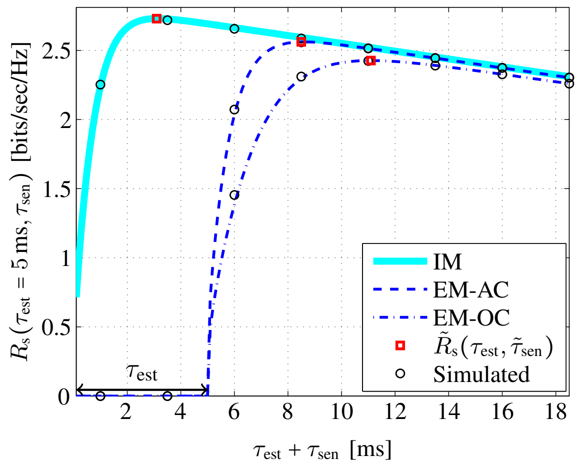

Fig. 6. Sensing-throughput tradeoff for the ideal and estimation models with $\gamma_{p,1} = -10\,\text{dB}$, $\tau_{est} = 5\,\text{ms}$ and $\kappa = 0.05$.

sensing time is established based on the average and outage constraint. In contrast to the ideal model, the sensing-throughput tradeoff substantiated by the estimation model, which incorporates the channel knowledge is qualified for characterizing the performance of IS.

Corollary 3: Herein, based on the estimation model, we establish a fundamental relation between estimation time (regulates the variation in the probability of detection according to the PU constraint), sensing time (represents the detector performance) and achievable throughput, this relationship is characterized as estimation-sensing-throughput tradeoff. Based on this tardeoff, we determine the suitable estimation $\tau_{est} = \tilde{\tau}_{est}$ and sensing time $\tau_{sen} = \tilde{\tau}_{sen}$ that achieves an optimum throughput $\tilde{R}_s(\tilde{\tau}_{est}, \tilde{\tau}_{sen})$ for the IS.

V. Numerical Results

Here, we investigate the performance of the IS based on the proposed model. To accomplish this: (i) we perform simulations to validate the expressions obtained, (ii) we analyze the performance loss incurred due to the estimation. In this regard, we consider the ideal model for benchmarking and evaluating the performance loss, (iii) we establish mathematical justification to the considered approximations. Although, the expressions derived using our sensing-throughput analysis are general and applicable to all CR systems, the parameters are selected in such a way that they closely relate to the deployment scenario described in Fig. 1. Unless stated explicitly, the following choice of the parameters is considered for the analysis, $f_s = 1\,\text{MHz}$, $h_{p,1} = h_{p,2} = -100\,\text{dB}, h_s = -80\,\text{dB}$, $T = 100\,\text{ms}$, $\bar{\text{P}}_d = 0.9$, $\kappa = 0.05$ $\sigma_w^2 = -100\,\text{dBm}$, $\gamma_{p,1} = -10\,\text{dB}$, $\gamma_{p,2} = -10\,\text{dB}$, $\gamma_s = 10\,\text{dB}$, $\sigma_x^2 = P_{Tx,PT} = -10\,\text{dBm}$ $P_{Tx,ST} = -10\,\text{dBm}$, $\mathbb{P}(\mathcal{H}_1) = 1 - \mathbb{P}(\mathcal{H}_0) = 0.2$, $\tau_{est} = 5\,\text{ms}$, $N_s = 10$ and $N_{p,2} = 1000$.

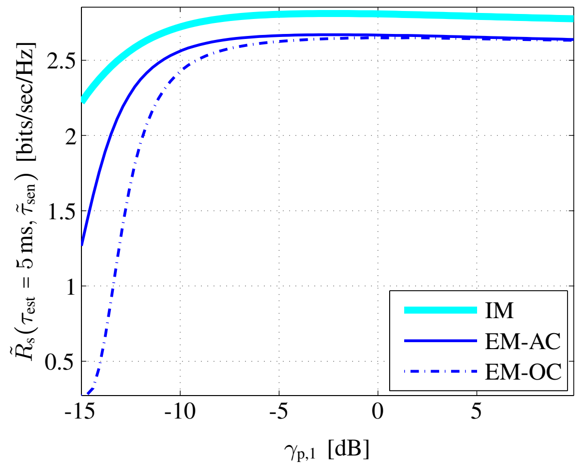

Fig. 7. Optimum throughput versus the $\gamma_{p,1}$ with $\tau_{est} = 5\,\text{ms}$.

Firstly, we analyze the performance of the IS in terms of sensing-throughput tradeoff corresponding to the ideal model (IM) and estimation model (EM) by fixing $\tau_{est} = 5\,\text{ms}$, cf. Fig. 6. In contrast to constraint on P_d for the ideal model, we employ average constraint (EM-AC) and outage constraint (EM-OC) for the proposed estimation model. With the inclusion of received power estimation in the frame structure, the ST procures no throughput at the SR for the interval τ_{est}. For the given cases, namely, IM, EM-AC and EM-OC, a suitable sensing time that results in an optimum throughput $\tilde{R}_s(\tau_{est} = 5\,\text{ms}, \tilde{\tau}_{sen})$ is determined. Hence, a performance degradation is depicted in terms of the optimum throughput, cf. Fig. 6. For $\kappa = 0.05$, it is observed that the outage constraint is more sensitive to the performance loss in comparison to average constraint. It is clear that the analysis illustrated Fig. 6 is obtained for a certain choice of system parameters, particularly $\gamma_{p,1} = -10\,\text{dB}$, $\tau_{est} = 5\,\text{ms}$ and $\kappa = 0.05$. To acquire more insights, we consider the effect of variation of these parameters on the performance of IS, subsequently.

Hereafter, for the analysis, we consider the theoretical expressions and choose to operate at suitable sensing time. Next, we determine the variations of the optimum throughput against the received signal to noise ratio $\gamma_{p,1}$ at the ST with $\tau_{est} = 5\,\text{ms}$, cf. Fig. 7. For $\gamma_{p,1} < -5\,\text{dB}$, the estimation model incurs a significant performance loss. This clearly reveals that the ideal model overestimates the performance of IS. Hence, it is perceived that despite loss in performance, the estimation model is capable of precluding interference at the PR, hence, assuring reliability to the system.

Upon optimizing the secondary throughput, it is interesting to analyze the variation of optimum throughput against the estimation time. Corresponding to the estimation model, Fig. 8 illustrates a tradeoff between the estimation time, the sensing time and the throughput, cf. Corollary 3. This can be explained

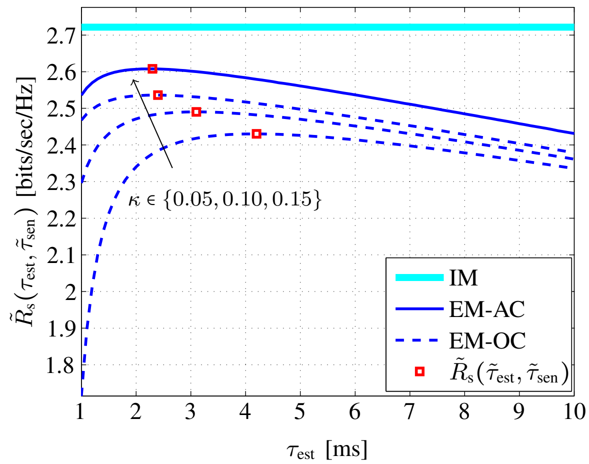

Fig. 8. Estimation-throughput tradeoff for the adjacent and outage constraint with $\gamma_{\mathrm{p},1} = -10\,\mathrm{dB}$, where the throughput is maximized over the sensing time, $\tilde{R}_{\mathrm{s}}(\tau_{\mathrm{est}}, \tilde{\tau}_{\mathrm{sen}})$. Estimation-throughput tradeoff is utilized to determine a suitable estimation time $\tilde{\tau}_{\mathrm{est}}$ that optimizes the throughput, $\tilde{R}_{\mathrm{s}}(\tilde{\tau}_{\mathrm{est}}, \tilde{\tau}_{\mathrm{sen}})$.

from the fact that low values of estimation time result in large variation in $\mathrm{P_d}$. To counteract and satisfy the average and outage constraints, the corresponding thresholds shift to a lower value. This causes an increase in $\mathrm{P_{fa}}$, thereby increasing the sensing-throughput curvature. As a result, the optimum sensing time is obtained at a higher value. However, beyond a certain value ($\tilde{\tau}_{\mathrm{est}}$), a further increase in estimation time slightly contributes to performance improvement and largely consumes the time resources. As a consequence to the estimation-sensing-throughput tradeoff, we determine the suitable estimation time that yields an optimum throughput $\tilde{R}_{\mathrm{s}}(\tilde{\tau}_{\mathrm{est}}, \tilde{\tau}_{\mathrm{sen}})$. Besides that, we consider the variation of optimum throughput for different values of the outage constraint, cf. Fig. 8. It is observed that for the selected the choice of κ, the outage constraint is stringent as compare to the average constraint, hence, results in a lower optimum throughput. Thus, depending on the nature of policy (aggressive or conservative) followed by the regulatory towards interference at the primary system, it is possible to define κ accordingly at the system design.

To procure further insights, we investigate the variations of expected $\mathrm{P_d}$ and $\mathrm{P_{fa}}$ against the estimation time. From Fig. 9a, it is noticed that the expected $\mathrm{P_d}$ corresponding to the outage constraint is strictly above the desired level $\bar{\mathrm{P}}_{\mathrm{d}}$ for all values of estimation time, however, for lower value of estimation time, this margin reduces. This is based on the fact that lower estimation time shifts the probability mass of $\mathrm{P_d}$, to lower value, cf. Fig. 3a. Besides that, based on the previous discussion, it was analyzed that $\mathrm{P_{fa}}$ accounts for a large contribution to the throughput. According to Fig. 9b, $\mathrm{P_{fa}}$ witnesses a large improvement in

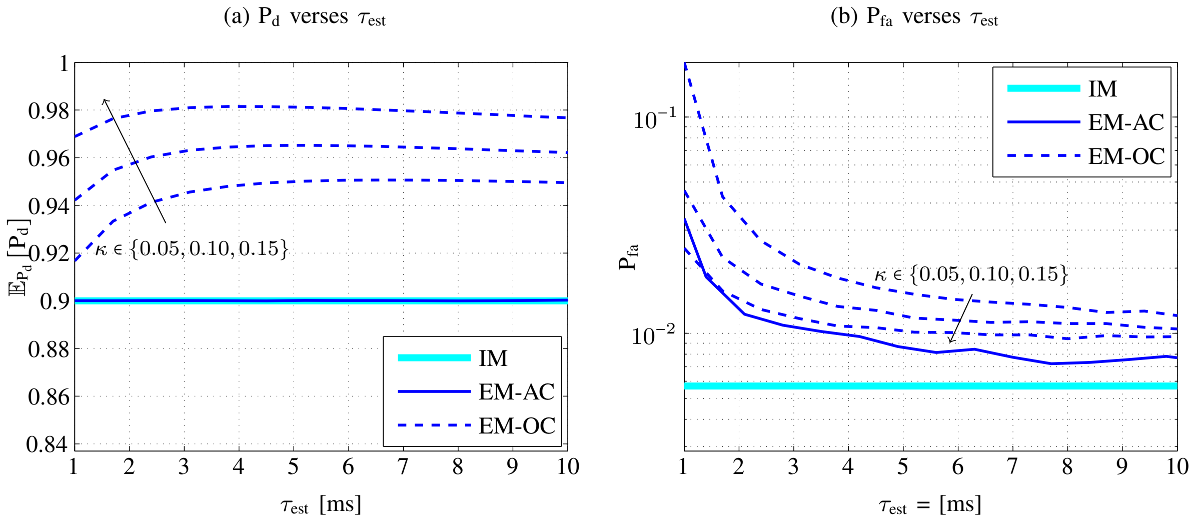

Fig. 9. Variation of $\mathbb{E}_{\mathrm{P_d}}[\mathrm{P_d}]$ and $\mathrm{P_{fa}}$ verses the τ_{est}, where the throughput is maximized over the sensing time, $\tilde{R}_{\mathrm{s}}(\tau_{\mathrm{est}}, \tilde{\tau}_{\mathrm{sen}})$.

performance in the regime $\tau_{\mathrm{est}} \leq 3\,\mathrm{ms}$, however, saturates in the regime $\tau_{\mathrm{est}} \geq 3\,\mathrm{ms}$, thus, provides further justification to the variation of $\tilde{R}_{\mathrm{s}}(\tau_{\mathrm{est}}, \tilde{\tau}_{\mathrm{sen}})$ against τ_{est} characterized as estimation-sensing-throughput tradeoff depicted in Fig. 8.

VI. Conclusion

In this paper, we have investigated the performance of cognitive radio as an interweave system from a deployment perspective. It has been argued that the knowledge of the interacting channels is a key aspect that enables the performance characterization of the interweave system in terms of sensing-throughput tradeoff. In this regard, a novel model that facilitates channel estimation and captures the effect of estimation in the system has been proposed. As a major outcome of the analysis, it has been justified that the existing model, illustrating an ideal scenario, overestimates the performance of the interweave system, hence, less suitable for deployment. Moreover, it has been indicated that the variation induced in the system, specially in the probability of detection may severely degrade the performance of primary system. To overcome this situation, average and outage constraints as primary user constraints have been employed. As a consequence, for the estimation model, novel expressions for sensing-throughput tradeoff based on the mentioned constraints have been established. Lastly, by analyzing the estimation-sensing-throughput tradeoff, suitable estimation time and sensing time that optimize the throughput at the secondary receiver have been determined. In our future work, we plan to extend the proposed analysis for the hybrid cognitive radio which combines the advantages of interweave and underlay techniques.

REFERENCES

[1] A. Kaushik, S. K. Sharma, S. Chatzinotas, B. Ottersten, and F. K. Jondral, "Sensing-Throughput Tradeoff for Cognitive Radio Systems with Unknown Received Power," in *10th International Conference on Cognitive Radio Oriented Wireless Networks and Communications (CROWNCOM)*, April 2015.

[2] J. Andrews *et al.*, "What Will 5G Be?" *IEEE Journal on Selected Areas in Communications*, vol. 32, no. 6, pp. 1065–1082, June 2014.

[3] Rappaport *et al.*, "Millimeter Wave Mobile Communications for 5G Cellular: It Will Work!" *IEEE Access*, vol. 1, pp. 335–349, 2013.

[4] J. Mitola and G. Q. Jr. Maguire, "Cognitive radio: making software radios more personal," *IEEE Personal Communications*, vol. 6, no. 4, pp. 13–18, August 1999.

[5] A. Goldsmith, S. Jafar, I. Maric, and S. Srinivasa, "Breaking Spectrum Gridlock With Cognitive Radios: An Information Theoretic Perspective," *Proceedings of the IEEE*, vol. 97, no. 5, pp. 894–914, May 2009.

[6] S. Sharma *et al.*, "Cognitive Radio Techniques under Practical Imperfections: A Survey," *IEEE Communications Surveys Tutorials*, vol. PP, no. 99, pp. 1–1, 2015.

[7] E. Axell, G. Leus, E. Larsson, and H. Poor, "Spectrum sensing for cognitive radio : State-of-the-art and recent advances," *IEEE Signal Processing Magazine*, vol. 29, no. 3, pp. 101–116, May 2012.

[8] H. Urkowitz, "Energy detection of unknown deterministic signals," *Proceedings of the IEEE*, vol. 55, no. 4, pp. 523 – 531, april 1967.

[9] V. Kostylev, "Energy detection of a signal with random amplitude," in *IEEE ICC*, vol. 3, 2002, pp. 1606–1610 vol.3.

[10] F. Digham, M.-S. Alouini, and M. K. Simon, "On the energy detection of unknown signals over fading channels," in *IEEE ICC*, vol. 5, May 2003, pp. 3575–3579.

[11] S. Herath, N. Rajatheva, and C. Tellambura, "Unified approach for energy detection of unknown deterministic signal in cognitive radio over fading channels," in *IEEE ICC Workshops*, June 2009, pp. 1–5.

[12] A. Mariani, A. Giorgetti, and M. Chiani, "Energy detector design for cognitive radio applications," in *2010 International Waveform Diversity and Design Conference (WDD)*, Aug 2010, pp. 000 053–000 057.

[13] E. Peh and Y.-C. Liang, "Optimization for cooperative sensing in cognitive radio networks," in *IEEE Wireless Communications and Networking Conference (WCNC)*, March 2007, pp. 27–32.

[14] Y.-C. Liang, Y. Zeng, E. Peh, and A. T. Hoang, "Sensing-Throughput Tradeoff for Cognitive Radio Networks," *IEEE Transactions on Wireless Communications,*, vol. 7, no. 4, pp. 1326–1337, April 2008.

[15] S. Sharma, S. Chatzinotas, and B. Ottersten, "A hybrid cognitive transceiver architecture: Sensing-throughput tradeoff," in *CROWNCOM*, Jun. 2014.

[16] H. Pradhan, S. Kalamkar, and A. Banerjee, "Sensing-throughput tradeoff in cognitive radio with random arrivals and departures of multiple primary users," *IEEE Communications Letters*, vol. 19, no. 3, pp. 415–418, March 2015.

[17] M. K. Simon and M. S. Alouini, *Digital Communication over Fading Channels: A Unified Approach to Performance Analysis*, 1st ed. New York: Wiley, 2000.

[18] A. Kaushik, M. R. Raza, and F. K. Jondral, "On the Deployment of Cognitive Relay as Underlay Systems," in *CROWNCOM*, Jun. 2014.

[19] M. Cardenas-Juarez and M. Ghogho, "Spectrum Sensing and Throughput Trade-off in Cognitive Radio under Outage Constraints over Nakagami Fading," *IEEE Communications Letters*, vol. 15, no. 10, pp. 1110–1113, October 2011.

[20] Y. Sharkasi, M. Ghogho, and D. McLernon, "Sensing-throughput tradeoff for OFDM-based cognitive radio under outage constraints," in *ISWCS*, Aug 2012, pp. 66–70.

[21] R. Tandra and A. Sahai, "SNR Walls for Signal Detection," *IEEE Journal of Selected Topics in Signal Processing*, vol. 2, no. 1, pp. 4–17, Feb 2008.

[22] M. Gans, "The effect of gaussian error in maximal ratio combiners," *IEEE Transactions on Communication Technology*, vol. 19, no. 4, pp. 492–500, August 1971.

[23] W. Gifford, M. Win, and M. Chiani, "Diversity with practical channel estimation," *IEEE Transactions on Wireless Communications*, vol. 4, no. 4, pp. 1935–1947, July 2005.

[24] ——, "Antenna subset diversity with non-ideal channel estimation," *IEEE Transactions on Wireless Communications*, vol. 7, no. 5, pp. 1527–1539, May 2008.

[25] R. Annavajjala and L. Milstein, "Performance analysis of linear diversity-combining schemes on rayleigh fading channels with binary signaling and gaussian weighting errors," *IEEE Transactions on Wireless Communications*, vol. 4, no. 5, pp. 2267–2278, Sept 2005.

[26] H. Suraweera, P. Smith, and M. Shafi, "Capacity limits and performance analysis of cognitive radio with imperfect channel knowledge," *IEEE Transactions on Vehicular Technology*, vol. 59, no. 4, pp. 1811–1822, May 2010.

[27] H. Kim, H. Wang, S. Lim, and D. Hong, "On the impact of outdated channel information on the capacity of secondary user in spectrum sharing environments," *IEEE Transactions on Wireless Communications*, vol. 11, no. 1, pp. 284–295, January 2012.

[28] A. Kaushik, S. K. Sharma, S. Chatzinotas, B. Ottersten, and F. K. Jondral, "Estimation-Throughput tradeoff for underlay cognitive radio systems," *IEEE ICC 2015 - Cognitive Radio and Networks Symposium (ICC'15 (12) CRN)*, Jun. 2015.

[29] A. Kaushik, M. Mueller, and F. K. Jondral, "Cognitive Relay: Detecting Spectrum Holes in a Dynamic Scenario," in *ISWCS*, Apr. 2013, pp. 1–2.

[30] T. Wang, Y. Chen, E. Hines, and B. Zhao, "Analysis of effect of primary user traffic on spectrum sensing performance," in *Communications and Networking in China, 2009. ChinaCOM 2009. Fourth International Conference on*, Aug 2009, pp. 1–5.

[31] L. Tang, Y. Chen, E. Hines, and M.-S. Alouini, "Effect of primary user traffic on sensing-throughput tradeoff for cognitive radios," *IEEE Transactions on Wireless Communications*, vol. 10, no. 4, pp. 1063–1068, April 2011.

[32] B. Zhao, Y. Chen, C. He, and L. Jiang, "Performance analysis of spectrum sensing with multiple primary users," *IEEE Transactions on Vehicular Technology*, vol. 61, no. 2, pp. 914–918, Feb 2012.

[33] S. Kay, *Fundamentals of Statistical Signal Processing: Detection theory*, ser. Prentice Hall Signal Processing Series. Prentice-Hall PTR, 1998.

[34] I. S. Gradshteyn and I. M. Ryzhik, *Table of Integrals, Series, and Products*, 6th ed. San Diego, CA: Academic Press., 2000.

[35] M. Abramowitz and I. A. Stegun, *Handbook of Mathematical Functions with Formulas, Graphs, and Mathematical Tables*, ninth Dover printing, tenth GPO printing ed. New York: Dover, 1964.

[36] F. W. J. Olver, D. W. Lozier, R. F. Boisvert, and C. W. Clark, Eds., *NIST Handbook of Mathematical Functions*. New York, NY: Cambridge University Press, 2010.